2022 Second International Conference on Advances in Electrical, Computing, Communication and Sustainable Technologies (ICAECT) | 978-1-6654-1120-2/22/$31.00 ©2022 IEEE | DOI: 10.1109/ICAECT54875.2022.9808038

Grid Tied Photovoltaic Based Electric Vehicle Charging Infrastructure

Mamta Gupta
Department of Electrical Engineering
Delhi Technological University
Delhi, India
mamtagupta_2k20psy10@dtu.ac.in

Aakash Kumar Seth
Department of Electrical Engineering
Delhi Technological University
Delhi, India
akrseth@gmail.com

Mukhtiar Singh
Department of Electrical Engineering
Delhi Technological University
Delhi, India
smukhtiar_79@yahoo.co.in

Abstract— **This paper presents detailed simulation of grid tied photovoltaic (PV) based an electric vehicle (EV) charging infrastructure. The EV charger can work in both modes of power flow i.e., grid to vehicle (G2V) and vehicle to grid (V2G), which can be employed in diverse load power requirement scenarios. The overall system uses various converters at each stage, boost converter for harnessing solar PV power, a bi-directional buck-boost converter for EV charging, and a voltage source converter (VSC) with LCL filter for integrating overall system with the grid. The controlling of DC-DC boost converter for extracting peak power output is done using maximum power point tracking (MPPT) technique. The controller associated with bidirectional buck-boost converter is used for controlling power flow of battery pack. Moreover, the controller of grid side bidirectional AC-DC converter is utilized for controlling DC-link voltage. The system presented in this paper contributes towards maximizing energy output from PV system with perturbation and observation (P&O), uninterrupted EV charging, enhancing grid performance and using EV as a form of energy storage system when required. Extensive simulation for various power flow modes have been performed to verify the aforementioned claims. The overall design and simulation work is executed in MATLAB/Simulink software and results are confirmed for various input conditions.**

Keywords—Photovoltaic, Vehicle to Grid, Grid to Vehicle, EV charging, Grid Power Support

I. INTRODUCTION

In the last couple of decades, the growing concern in the energy sector is mainly due to continuous depletion of fossil fuels and emission of carbon di oxide which leads to green-house effect. For sustainable management of conventional resources and for minimizing hazardous environmental condition, in the field of alternate energy sources further research and development is required. Solar powered energy is one of the most widely used non-conventional energy, as it is abundant, inexhaustible, free and clean [1].

One of the major sectors using fossil fuel and natural gas is the transportation sector, hence battery electric vehicle was developed as an alternative to Internal Combustion (IC) engines, for reducing emission of CO2 and to limit the use of fossil fuel. Integration of EV with grid can also provide other ancillary services like regulation of voltage and frequency, peak shaving, can act as a virtual power plant and regulated spinning reserve with the smart grid [2]-[4].

Moreover, integration of EV on a huge scale and its unregulated connection into the power distribution system might poses various problem such as rising peak demand, harmonics, voltage imbalance and current distortion etc. [5]. Another issue is that no emission EVs are majorly charged using electricity grid, where the major concentration of fuel mix comes from conventional sources, hence PV powered EV charging is a sustainable option for long term [6]. Interconnection of solar PV system with EV charging in a coordinated manner mitigates impact of solar PV generation on power grid. However, PV integrated system with EV leads to system complexity and to avoid issues related to solar power fluctuation, there is a need of integration of PV with grid and other multifunctional operating sources for reliable operation of EV charging [6]-[7].

There are three charging levels for EV [8]. Level 1 charging consist of an on-board charger with 120 – 240 V AC and 15 A of maximum current. The Level 2 charging consist of an on-board charger of voltage level 240 V with maximum charging current of 40 A. Level 3 consist of an off-board charger with 200-800 V and 250 A of maximum current.

In the literature [9]-[11], various topologies of grid integrated PV systems have been discussed. An adjustable DC-link with two stage grid tied solar PV system is presented [12], and an elimination of one stage leads to single stage topology having their own benefits and drawbacks. Topologies are also dependent on certain other factors such as isolation, power level requirement and controlling strategy. In [1], the elimination of boost converter is presented, here DC bus directly connects solar PV array with VSC, allowing VSC to harness the peak power out of solar PV array.

Several control strategies have already been presented in literature for different power converters mainly includes Proportional-Integral (PI) control, Proportional-Resonant (PR) control, Repetitive control (RC), Model Predictive Control (MPC) etc. [13]-[16]. In this work, boost converter harnesses peak power out of PV array, which is further interconnected with DC link of VSC for AC-DC conversion. The EV battery charger is interfaced at DC link with the help of DC-DC bi-directional buck-boost converter. The control algorithm prioritizes energy sources utilization based on solar power generation and EV charging requirement. Firstly, it utilizes solar power for EV charging and in case of less availability or over power generation remaining power is taken from or fed to grid respectively. EV can also be used as a form of storage system and during peak load time it can supply energy back to grid. During unavailability of solar power, EV and grid can act as an isolated system having both V2G and G2V mode.

The overall system configuration as shown in Fig. 1. is designed in MATLAB/Simulink software, where total seven power flow modes from mode 1 to mode 7, which has been discussed in Table II., is simulated to validate controller performance upon various input conditions and load power requirements.

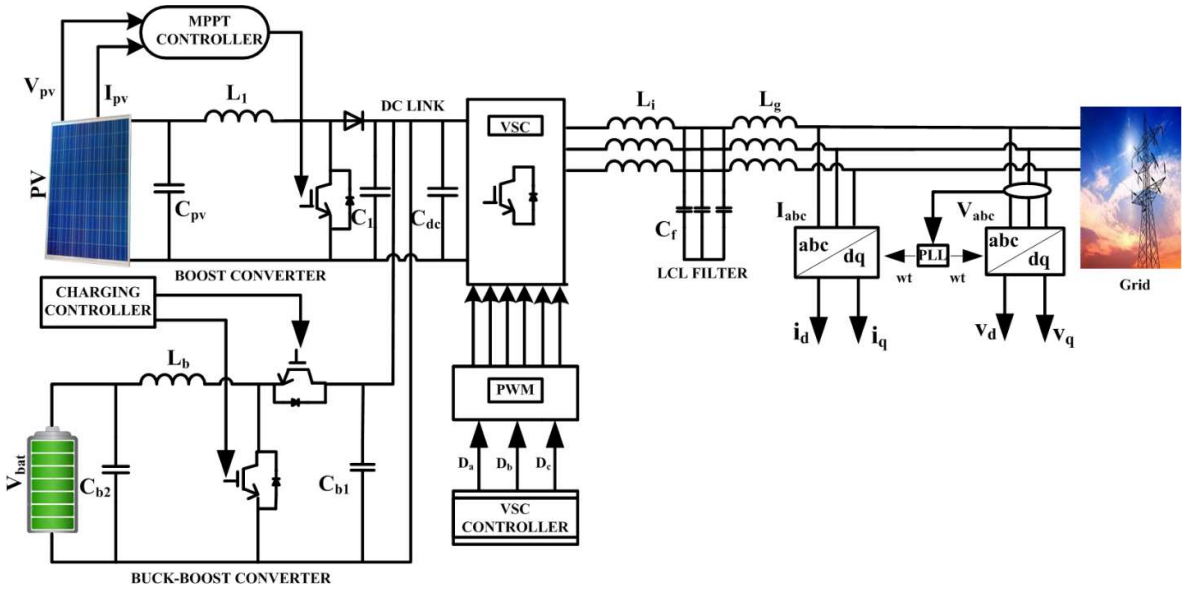

Fig. 1. Overall system configuration

II. SYSTEM DESCRIPTION

The complete system architecture is shown in Fig. 1. The system consists of PV source, grid and EV charging station.

A. Solar PV cell model

Fig. 2. shows equivalent electric circuit model of PV cell which is obtained after analyzing its terminal characteristic, which is further utilized to design photovoltaic systems. The terminal equation that governs the output voltage-current performance characteristic of PV cell is as follows:

$$I_D = I_O\left(e^{\frac{V+IR_{se}}{nVt}} - 1\right) \quad (1)$$

$$I = I_{sc} - I_O\left(e^{\frac{V+IR_{se}}{nVt}} - 1\right) - \frac{V+IR_{se}}{R_{sh}} \quad (2)$$

Where I_{sc} represents the photo electric current proportional to the total amount of perpendicular solar energy incident on solar cell surface, I_o represents the reverse saturation current which is dependent on doping and temperature of p-n junction diode; R_{sh} and R_{se} implies shunt and series resistance present due to nonlinearity in PV characteristic; n denotes the diode ideality factor and V_T represents the thermal voltage.

The above equation is an acausal equation but in practice diode is not ideal hence it has the junction capacitance which takes care of the causality problems.

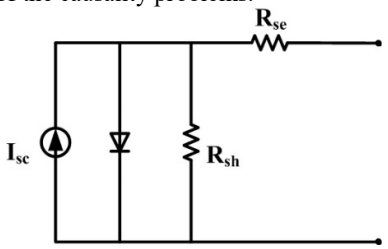

Fig. 2. Electric equivalent PV cell model.

Under different irradiation levels, characteristic of *I-V*, *P-V* is drawn, which is depicted in Fig. 3. The nonlinearity in PV cell characteristic indicates that, the unique *I-V* characteristic results in output current which is constant over a wide voltage range until it extends to a point from where it begins to drop exponentially, giving rise to the concept of maximum power point which has to be tracked for exporting peak power out of solar array.

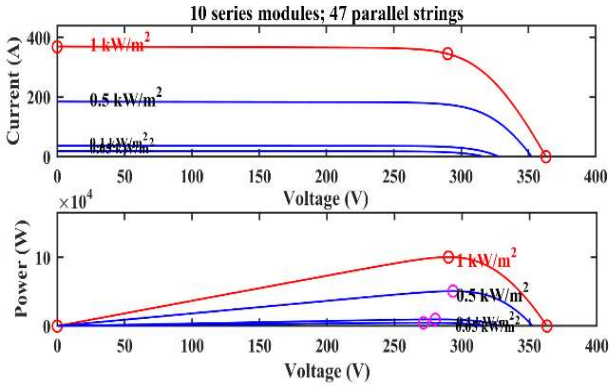

Fig. 3. PV array characteristic.

B. Boost Converter MPPT control

The main function of DC-DC boost converter is to rise the source side solar PV array voltage to load terminal by adjusting the duty cycle. This duty cycle, for maximum power is maintained by MPPT techniques. Among several MPPT techniques, Perturbation and observation (P&O) method is most widely implemented because of the limited number of parameters required, simplicity in its structure and ease in calculation. The parameter required to track MPP is current and voltage of PV panel as input values, which implies the association between output power and terminal voltage. This method iteratively perturbs, observes and generates output power to track maximum power point. If at certain PV module operating $\frac{\Delta P}{\Delta V} > 0$ then the perturbation of PV module output voltage should be increased toward MPP, if PV module operating point $\frac{\Delta P}{\Delta V} < 0$ then the perturbation of PV module output voltage should be decreased toward MPP. If the status of certain point is $\frac{\Delta P}{\Delta V} = 0$ then that point is the

point of maximum power. The MPPT flow chart is shown in Fig. 4.

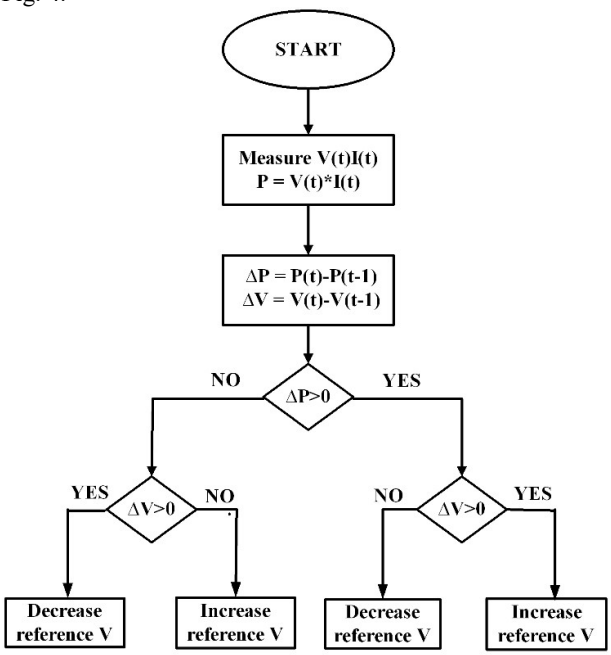

Fig. 4. P & 0 flow chart.

For boost converter control through MPPT, PV current and voltage is first sensed and passed through MPPT to generate V_{ref} which is the reference voltage for tracking MPP, error signal is generated by comparing V_{ref} with PV voltage, which is then passed to the PI controller , which will further generate signal having the required duty ratio, The output PWM signal is a result of comparing this generated signal with the carrier signal for the purpose of getting the required switching pulses for the boost converter as shown in Fig. 5.

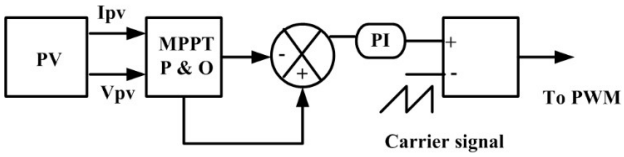

Fig. 5. MPPT control block diagram.

C. *Voltage source converter configuration*

The converter implemented for PV to grid connection is bi-directional three phase AC to DC converter with sine pulse width modulation technique. The bidirectional power flow is important for this work as it allows power flow in both forward and reverse direction depending upon load requirement. For such an application appropriate control strategy of power switches of converter is required.

Design of LCL filter

The PV inverter section, on the DC input side consist of PV panel and DC link capacitor and on the output AC side consist of an LCL filter interfaced with the grid. PV panel generated voltage must always maintain a DC-link voltage greater than the peak AC voltage at all time. Switching harmonics created by PWM must be reduced to improve the quality of power provided to local loads and that injected into the grid, for improving this quality, filters are required. There are many filter topologies for example *L* , *LC* and *LCL* filter etc., among various filter topologies *LCL* filter is the most suitable for providing better attenuation and coupling capability.

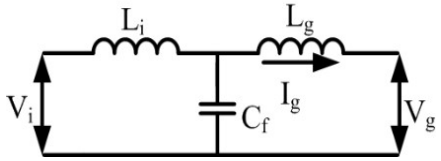

Fig. 6. Single phase equivalent model of LCL filter.

LCL filter has good ripple attenuation capability but can cause resonance related disturbance hence selection of filter components needs to be precise. For the design of filter, selecting filter components depends on several factors. Device constraint, cost and thermal consideration etc. influence switching frequency selection. The switching frequency of 10 kHz is chosen in this case.

The fundamental and switching frequency both must be very well separated from resonant frequency for its selection. The transfer function of LCL filter neglecting damping, all higher order harmonics condition, and by setting condition of $V_g = 0$ as shown in Fig. 6. is as follows:

$$\frac{Ig(s)}{Vi(s)} = \frac{1}{S^3 Li\ Lg\ C_f + S(Li + Lg)} \tag{3}$$

The capacitance value is determined based on reactive power requirement of capacitor. Due to this reactive power, overall output power factor is reduced causing large current to flow from IGBTs and L_i. The formula of capacitor C_f as shown in eq. (4) can be derived, with the limitation of reactive power requirement, keeping its value below 5% of inverter's rated output power.

$$C_f = \frac{0.05 * S}{v^2 * 2 * pi * f} \tag{4}$$

For the minimization of ripple current flowing through switching IGBTs inverter side inductor is required. The total change in current during the overall cycle is expressed as:

$$\Delta i = \frac{V_{dc}}{F_{sw} * 2L_i}(1 - M_r \sin \omega_0 t) M_r sinw_0 t \tag{5}$$

Where F_{sw} is the switching frequency for the IGBT's, V_{dc} represents input DC-link voltage , ω_0 refers to the fundamental angular frequency and modulation index is represented by M_r.

Considering the design constraints, 10 % ripple variation of rated current is allowed, for designing of inductor maximum value of ripple content is calculated, after further simplification and by putting appropriate value of ω_0, L_i follows the equation:

$$L_i = \frac{V_{dc}}{8 * F_{sw} * \Delta i_{max}} \tag{6}$$

The use of grid side inductor is to mitigate and keep current harmonics and total harmonic distortion (THD) under specified IEEE standards. The following equation gives the minimum value of L_g:

$$L_g = \frac{1}{L_i C \omega_n^2 - 1}\left(L_g - \frac{\left|V_g(j\omega_n)\right|}{\omega_n \mu_n I_g}\right) \tag{7}$$

For this computation we require to obtain frequency spectrum of voltage $\left|V_g(j\omega_n)\right|$. The angular frequency (ω_n)

of dominant harmonic must be determined from that equation. The estimated harmonic proportion of the filter output current is μ_n.

D. Battery charger configuration

DC bus links EV batteries to off board charger. DC-DC converter is the basic building block and act as an interface to above battery charger configuration. The converter configuration as shown in Fig. 1. consist of two IGBT switches which always operate in complimentary fashion.

It permits power to flow in both directions, resulting in two modes of operation: buck and boost. When PV is incapable of operating it provides V2G operation hence EV acts as an auxiliary power supply leading to different modes of operation. The equation governing the above two operations are as follows:

Boost mode: $V_H = \frac{V_L}{1-D}$ (8)

Buck mode: $V_H = \frac{V_L}{D}$ (9)

V_H and V_L denotes voltages on high voltage and low voltage ends.

III. CONTROL DEVELOPMENT

A. Voltage source converter control

The PI based controller design of VSC is depicted in the Fig. 7. The controller ensures DC-link voltage regulation. It is required for the reference value to be constant in its steady state for the necessary integral action of a PI based current controller to provide zero steady state error control, this can be achieved by applying Clarke's and park's transformation which is used to transform AC based current quantities into DC quantities and hence simple PI controller gives good result. The phase looked loop (PLL) is used to calculate ωt which maintains the synchronization between inverter current and grid voltage.

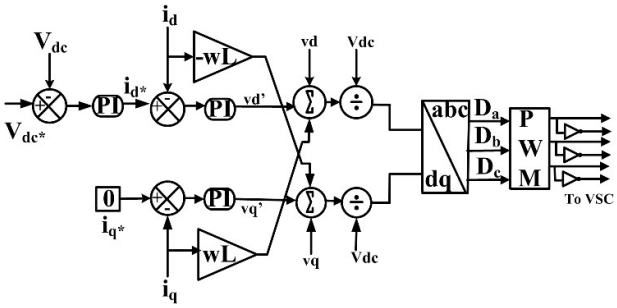

Fig. 7. VSC decoupled current controller.

Since, PV based grid system is in combination with EV charging system, multimode controller combinations are required. Two control loops is used in this PWM based technique i.e. an outer slower voltage loop which is used to regulate DC link voltage and an inner fast current loop for controlling *dq* axis current (i_d and i_q). Since, the *d* and *q* axis values are interconnected, controlling the active and reactive flow of power into the grid requires the use of two PI controllers. The DC link voltage is regulated by the PI controller, by minimizing the difference between the reference and actual voltage values, which further act as a reference for the *d* axis current (i_d^*). The line current vector must be aligned with the line voltage vector to achieve the condition of Unity Power Factor (UPF), hence the *q* axis current reference is set to zero ($i_q^* = 0$). The expression for *dq* axis current is as follows:

$$\frac{di_d}{dt} = v_d - k_p v_d{}' - k_i i_d + wLi_q/L \quad (10)$$

$$\frac{di_q}{dt} = v_q - k_p v_q{}' - k_i i_q - wLi_d/L \quad (11)$$

Where *L* is the line inductance and *w* is the grid's angular frequency. In addition, ignoring inverter losses, the equation for active and reactive power is as follows:

$$P = \frac{3}{2} Re\{v^{dq}(i^{dq})^*\} = \frac{3}{2}(v_d i_d + v_q i_q) \quad (12)$$

$$Q = \frac{3}{2} Im\{v^{dq}(i^{dq})^*\} = \frac{3}{2}(v_q i_d - v_d i_q) \quad (13)$$

Since, $i_q^* = 0$ so voltage vector is aligned with *d* axis, we get:

$$P = \frac{3}{2}(v_d \times i_d) \quad (14)$$

$$Q = 0 \quad (15)$$

B. Battery charger control

Fig. 8. depicts a PI controller-based constant current control that is used to control the charging and discharging of an electric vehicle battery. Depending on the direction of power flow, buck and boost mode is operated. Buck mode is used to charge the battery if the SOC is less than the threshold value, and boost mode is used to operate V2G if the SOC is larger than the threshold and based on required load power demand on grid.

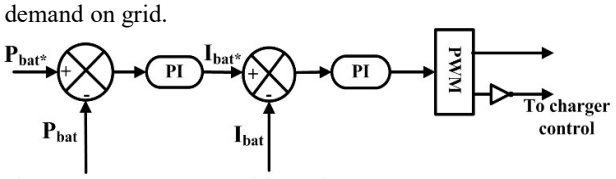

Fig. 8. Constant current control for EV battery.

The operation of a DC-DC bi-directional converter is determined by the amount of PV power generated, the state of charge (SOC) of the electric vehicle battery, and the load demand of the power grid. For proper operation of different modes, I_{bat} and P_{bat} are the two quantities which needs to be controlled by the controller, therefore two PI controllers are required. For outer loop battery actual power is compared with the reference power to obtain the signal which will be further compared with battery current to generate switching pulses i.e. D. Based on the generated power reference and measured power, decision is made by the controller leading to operation of battery charging (buck) and battery discharging/V2G (boost) mode.

$$I_{bat}{}^* = (k_{p1} + \frac{k_{i1}}{s}) * (P_{bat}{}^* - P_{bat}) \quad (16)$$

$$D = (k_{p2} + \frac{k_{i2}}{s}) * (I_{bat}{}^* - I_{bat}) \quad (17)$$

IV. RESULTS AND DISCUSSION

An integrated solar PV based EV charging system consisting of various controllers, power electronics converters as shown in Fig. 1. is executed in *MATLAB/Simulink* environment. Table I. enumerates the system parameters of the above model.

TABLE I. System parameters

PARAMETER	SYMBOL	VALUES
PV Power	P_{pv}	100 kW
Open circuit voltage of PV array	V_{oc}	363 V
DC link voltage	V_{dc}	600 V
Boost inductor	L_1	1.45 mH
Boost capacitor	C_1	3227 µF
Battery voltage	V_{bat}	350 V
Battery SOC	soc	50 %
Buck boost inductor	L_b	4 mh
Buck boost capacitor	C_{b1}	100 µF
Grid voltage	V_{grid}	400 V
Grid frequency	f	50 Hz
Switching frequency	f_{sw}	10 kHz
Filter inductor	L_i, L_g	500 mH
Filter capacitor	C_f	100 µF

To verify the performance claim of controllers, different modes of power flow as shown in Table II. are obtained depending on PV generated power, EV charging/discharging state, and grid power requirement. The PV system gives maximum power output of 100 kW and power varies according to irradiance condition 1000 $\frac{W}{m^2}$ – 500$\frac{W}{m^2}$ –1000 $\frac{W}{m^2}$ – 0 $\frac{W}{m^2}$ pertaining to different modes as shown in Fig. 9 (a). The DC-link voltage is maintained at its reference value of 600 V as inferred form Fig. 10.

TABLE II. SIMULATION VALUES

# MODE	IRRADIATION $\frac{W}{m^2}$	P_{PV} kW	P_{bat} kW	P_{grid} kW
1	1000	100	50	-50
2	500	48	80	32
3	500	48	48	0
4	1000	100	-50	-150
5	1000	100	0	-100
6	0	0	50	50
7	0	0	-50	-50

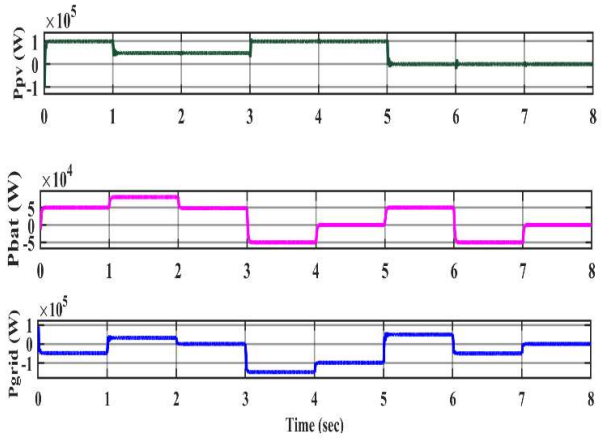

Fig. 9 (a) Solar PV generated power (b) Battery power waveform during charging/discharge mode (c) Grid active power (P_{grid}).

The power for solar PV, battery and grid active power for different modes of operation are enumerated in Table II. and shown in Fig. 9. During mode 1 generated PV power is used for charging of EV battery and power which is remaining is absorbed by the grid. Mode 2 shows EV charging through PV and grid both i.e. G2V mode is also shown here which will be required in case of increased EV charging demand and during the case in which PV is not sufficient enough to meet EV load demand. Mode 3 shows PV based EV charger which is isolated from grid. During the case of increase load demand on grid, mode 4 can be used where EV is acting as a storage system i.e. V2G operation and where both PV and EV are supplying power to meet the grid load demand. Mode 5 shows PV grid system isolated from EV. During mode 6 and mode 7, PV is isolated from EV and grid system, here G2V and V2G operations are shown respectively.

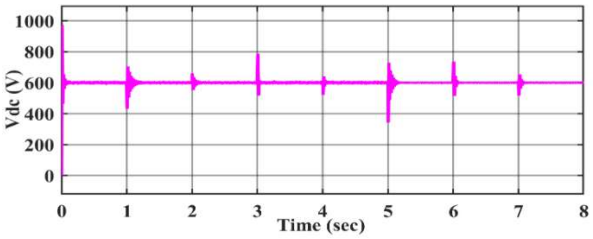

Fig. 10. DC link voltage.

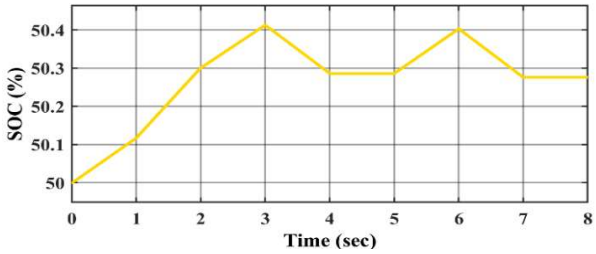

Fig. 11. SOC of battery.

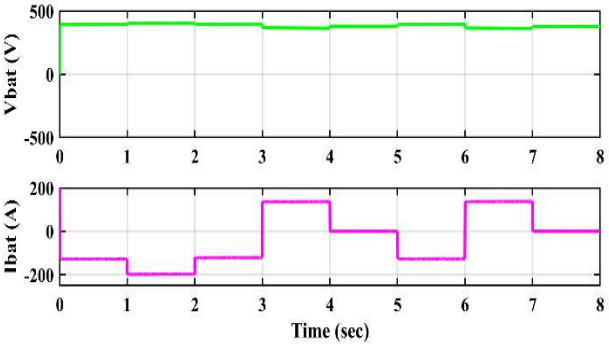

Fig. 12. Simulation result of battery voltage V_{bat} and battery current I_{bat}.

SOC, battery voltage (V_{bat}) and battery current (I_{bat}) are shown in Fig. 11 and 12 respectively. During mode 1 2 3 and 6 battery current is negative and battery power is positive which signifies battery charging state and in mode 4 and 7 battery current is positive and battery power is negative which signifies battery discharging state. Mode 5 is showing no action on EV. Battery voltage value is positive during all the stages. Battery SOC is increasing in mode 1 2 3 6 and decreasing in mode 4 and 7 signifying EV charging and discharging respectively. SOC is increasing faster in mode 2 which means more power is supplied to the battery in this mode compared to other modes.

Fig. 13 (a) and (b) shows instantaneous grid voltage and current. Mode 2 and 6 follows Fig. 13 (a) shows same phase between voltage and current and Fig. 9 (c). also signifies positive power for this modes i.e. power is supplied by the grid in this mode. Mode 1 4 5 7 follows Fig. 13 (b) and shows voltage and current in opposite phase and Fig. 9 (c). also

showing negative power for all this modes i.e. power is absorbed by the grid in this case.

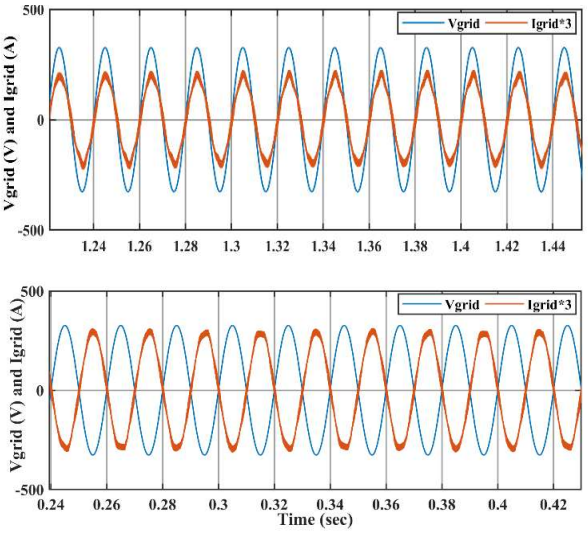

Fig. 13. Simulation results of instantaneous grid voltage and current during (a) mode 2 and 6 is in same phase and (b) and during mode 1, 4, 5 and 7 in out of phase.

V. Conclusions

In this work detailed modelling and simulation of grid tied PV based EV charging system has been carried out. The maximum power out of PV array is extracted with the help of DC-DC boost converter. The system is modelled to charge or discharge EV based on PV power availability, EV charge state and grid requirement using bi-directional converters. To verify the performance of controllers simulation for various modes have been carried out. This model is cost-effective and simple in design, and it supports PV power efficiency, continuous EV charging, and enhancement in grid power flow under a variety of load demand scenarios. Moreover, this model shows that the grid power quality will not be impacted in any of the power flow mode.

VI. References

[1] A. Verma, B. Singh, A. Chandra and K. Al-Haddad, "An Implementation of Solar PV Array Based Multifunctional EV Charger," *2018 IEEE Transportation Electrification Conference and Expo (ITEC)*, 2018, pp. 531-536, doi: 10.1109/ITEC.2018.8450191.

[2] L. Cheng, Y. Chang and R. Huang, "Mitigating Voltage Problem in Distribution System With Distributed Solar Generation Using Electric Vehicles," IEEE Trans. Sustainable Energy, vol. 6, no. 4, pp. 1475-1484, Oct. 2015, doi: 10.1109/TSTE.2015.2444390.

[3] M. Brenna, F. Foiadelli and M. Longo, "The Exploitation of Vehicle-to Grid Function for Power Quality Improvement in a Smart Grid," IEEE Trans. Intelligent Transportation Systems, vol. 15, no. 5, pp. 2169-2177, Oct. 2014, doi: 10.1109/TITS.2014.2312206.

[4] N. Saxena, I. Hussain, B. Singh and A. L. Vyas, "Implementation of a Grid-Integrated PV-Battery System for Residential and Electrical Vehicle Applications," in *IEEE Transactions on Industrial Electronics*, vol. 65, no. 8, pp. 6592-6601, Aug. 2018, doi: 10.1109/TIE.2017.2739712.

[5] L. Wang, Z. Qin, T. Slangen, P. Bauer and T. van Wijk, "Grid Impact of Electric Vehicle Fast Charging Stations: Trends, Standards, Issues and Mitigation Measures - An Overview," in *IEEE Open Journal of Power Electronics*, vol. 2, pp. 56-74, 2021, doi: 10.1109/OJPEL.2021.3054601.

[6] A. Verma and B. Singh, "Control and Implementation of Renewable Energy Based Smart Charging Station Beneficial for EVs, Home and Grid," *2019 IEEE Energy Conversion Congress and Exposition (ECCE)*, 2019, pp. 5443-5449, doi: 10.1109/ECCE.2019.8913253.

[7] B. Singh, A. Verma, A. Chandra, and K. Al-Haddad, "Implementation of Solar PV-Battery and Diesel Generator Based Electric Vehicle Charging Station," IEEE Transactions on Industry Applications, vol. 56, no. 4, pp. 4007-4016, 2020, doi: 10.1109/TIA.2020.2989680.

[8] S. Chalia, A. K. Seth and M. Singh, "Electric Vehicle Charging Standards in India and Safety Consideration," *2021 IEEE 8th Uttar Pradesh Section International Conference on Electrical, Electronics and Computer Engineering (UPCON)*, 2021, pp. 1-6, doi: 10.1109/UPCON52273.2021.9667649.

[9] A. Narula and V. Verma, "Dual Port Impedance Converter for PV – Battery fed Remote Telecom Towers," 2018 IEEE 4th Southern Power Electronics Conference (SPEC), 2018, pp. 1-7, doi: 10.1109/SPEC.2018.8636089.

[10] H. Saxena, A. Singh and J. N. Rai, "Application of Time Delay Recurrent Neural Network for Shunt Active Power Filter in 3-Phase Grid-tied PV System," 2019 National Power Electronics Conference (NPEC), 2019, pp. 1-6, doi: 10.1109/NPEC47332.2019.9034769.

[11] M. O. Badawy and Y. Sozer, "Power Flow Management of a Grid Tied PV-Battery System for Electric Vehicles Charging," in *IEEE Transactions on Industry Applications*, vol. 53, no. 2, pp. 1347-1357, March-April 2017, doi: 10.1109/TIA.2016.2633526.

[12] C. Jain and B. Singh, "An Adjustable DC Link Voltage-Based Control of Multifunctional Grid Interfaced Solar PV System," in *IEEE Journal of Emerging and Selected Topics in Power Electronics*, vol. 5, no. 2, pp. 651-660, June 2017, doi: 10.1109/JESTPE.2016.2627533.

[13] A. K. Seth and M. Singh, "Resonant controller of single-stage off-board EV charger in G2V and V2G modes," in IET Power Electronics, vol. 13, no. 5, pp. 1086-1092, 8-4-2020.

[14] A. K. Seth and M. Singh, "Second-Order Ripple Minimization in Single-Phase Single-Stage Onboard PEV Charger," in *IEEE Transactions on Transportation Electrification*, vol. 7, no. 3, pp. 1186-1195, Sept. 2021, doi: 10.1109/TTE.2021.3049559.

[15] T. He, J. Zhu, D. D. Lu and L. Zheng, "Modified Model Predictive Control for Bidirectional Four-Quadrant EV Chargers With Extended Set of Voltage Vectors," in IEEE Journal of Emerging and Selected Topics in Power Electronics, vol. 7, no. 1, pp. 274-281, March 2019, doi: 10.1109/JESTPE.2018.2870481.

[16] I. Jayathilaka *et al*., "DQ Transform Based Current Controller for Single-Phase Grid Connected Inverter," *2018 2nd International Conference On Electrical Engineering (EECon)*, 2018, pp. 32-37, doi: 10.1109/EECon.2018.8541004.